AIChE WILEY InterScience DISCOVER SOMETHING GREAT

Solution Technique for Pure-Component Phase Equilibria Near the Critical Point

L. N. Stapley and K. D. Luks
Dept. of Chemical Engineering, University of Tulsa, Tulsa, OK 74104

DOI 10.1002/aic.10751
Published online December 21, 2005 in Wiley InterScience (www.interscience.wiley.com).

An iterative technique is presented for determining pure-component phase equilibrium that essentially does not depend on initiation. The technique uses both the real and the complex conjugate root information obtained from the analytical solution to cubic equations of state to extend substantially the domain of convergence. The technique is robust and effective close to the critical point. © 2005 American Institute of Chemical Engineers *AIChE J,* 52: 1594–1599, 2006
Keywords: phase equilibrium, equation-of-state, complex domain

Introduction

A classic problem in equation-of-state (EOS) thermodynamics is finding the vapor–liquid saturation pressure P at $T < T_C$, for a pure component, using a cubic EOS such as the van der Waals EOS or more recent descendents such as the Soave–Redlich–Kwong EOS[1] (hereafter, "SRKEOS") and the Peng–Robinson EOS,[2] which are two of the more popular of many variants. The Second Law of thermodynamics dictates that pure-component vapor–liquid equilibrium is governed by the following equations:

$$\begin{aligned} T_g &= T_l \\ P_g &= P_l \\ \mu_g &= \mu_l \end{aligned} \tag{1}$$

where $\mu = \mu(P, T)$ is the chemical potential function, which is the molar Gibbs energy G for pure-component systems. Experiment presents this first-order phase transition in thermodynamic phase space with a discontinuity in the molar volume v in P–v space at a given $T < T_C$ (see Figure 1a). Given that

$$v = \left(\frac{\partial \mu}{\partial P}\right)_T \tag{2}$$

one also sees a discontinuity in the slope of μ in μ–P space at the phase-transition point (see Figure 1b).

Cubic equations of state, such as the van der Waals EOS and the above-mentioned descendent models, offer a homogeneous description of fluid properties. The geometry of the cubic EOS differs from the experimental picture in that it presents a continuous "van der Waals loop" in pressure–volume space, a mathematical artifice of the homogeneous nature of the EOS (see Figure 2a). This artifice is traditionally exploited by means of Maxwell construction, wherein it is recognized that along an isotherm $T < T_C$, the chemical potential function changes as

$$d\mu = v dP \tag{3}$$

By plotting μ vs. P for a subcritical isotherm, the first-order vapor–liquid phase transition can be mathematically identified as the self-intersection of the isotherm (see Figure 2b). The pressure at the intersection point in Figure 2b is equivalently the pressure (horizontal line) that divides the van der Waals loop in Figure 2a into equal areas. This pressure, when inserted into the cubic EOS produces three real volume roots, the largest of which is the saturated vapor molar volume and the smallest, the saturated liquid volume. As can be seen from Figure 2b, these two saturated states have the same value of the chemical potential function μ, whereas the intermediate molar volume root has a value of $\mu > \mu_g = \mu_l$. Because all three states are at the same (T, P), the Second Law dictates that the intermediate root be discarded. (Similarly, because the slope of the isotherm in Figure 2a is positive, the intermediate state is characterized by an isothermal compressibility $\kappa_T < 0$, which

Correspondence concerning this article should be addressed to K. D. Luks at kraemer-luks@utulsa.edu.

© 2005 American Institute of Chemical Engineers

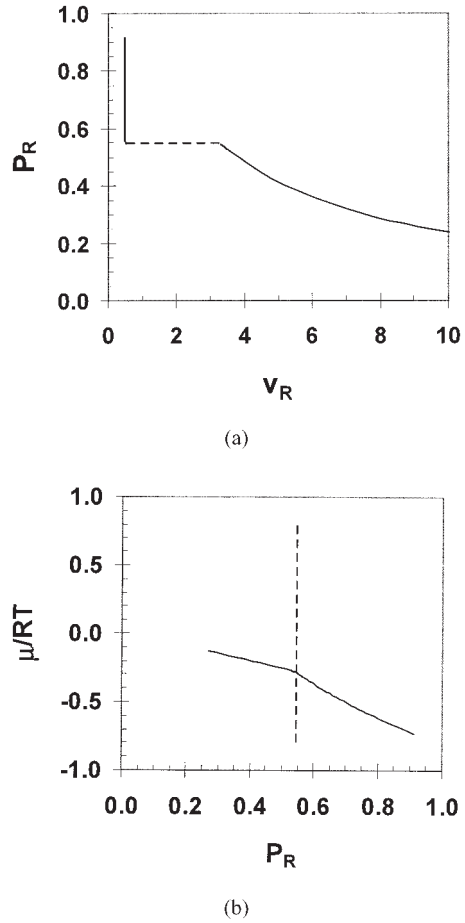

Figure 1. (a) Experimental reduced pressure P_R as a function of reduced volume v_R at $T_R = 0.90$ for a pure fluid with $\omega = 0$; (b) experimental reduced residual chemical potential function μ/RT as a function of reduced pressure P_R at $T_R = 0.90$ for a pure fluid with $\omega = 0$.

means that the state is intrinsically unstable.) After applying Maxwell construction and identifying the saturated state (T, P, v_g, v_l), one customarily ignores the loop portion of the cubic EOS, that between v_g and v_l, because it has no thermodynamic (long-time limit) analog in nature.

The aforementioned Figures 2a and 2b are from the homogeneous SRKEOS for a perfect fluid ($\omega = 0$) at a reduced temperature $T_R = 0.90$. The pressure domain of the EOS having three real molar volume roots extends over a sizable range. The three-real-molar-volume-root domain is present at all subcritical temperatures for a pure-component system, shrinking in size with increasing T_R, and vanishing at the critical point $T_R = 1$. Figures 3a and 3b are analogous to Figures 2a and 2b for the same SRKEOS fluid at $T_R = 0.99$.

There are a variety of strategies that can be used to find the state satisfying the Eq. 1 system for a homogeneous EOS at a given $T_R < 1$. The EOS problem, which is highly nonlinear, is generally solved by using Maxwell construction in some form or other, which in turn requires identifying certain features of the van der Waals loop artifice. For example, finding the pressure maximum and minimum in the loop provides bounds for the saturation pressure being sought. If one solves for these extremum pressures, one can initiate an iterative search with an intermediate pressure and, in principle, numerically navigate within the three-real-root region of the EOS in μ–P space to find the self-intersection point and its [saturation] pressure. However, finding the extremum pressures may pose a problem as $T_R \rightarrow 1$, where their values and their locations are close together along the volume coordinate, and the intermediate unstable portion of the loop flattens. (Cubic equations such as van der Waals, Soave–Redlich–Kwong, and Peng–Robinson offer a quartic equation for the z values of the pressure extrema that—with some patience—can be solved analytically.) Furthermore, success of the subsequent iterative search for $z \rightarrow P$ at equilibrium depends on staying within the three-real-root domain so that the self-intersection of μ-branches (as shown in Figure 3b) can be calculated. We stress here that identification of the three-real-root domain and subsequent restriction of an iterative search to this domain can be challenging when the domain becomes very small at $T_R \rightarrow 1$.

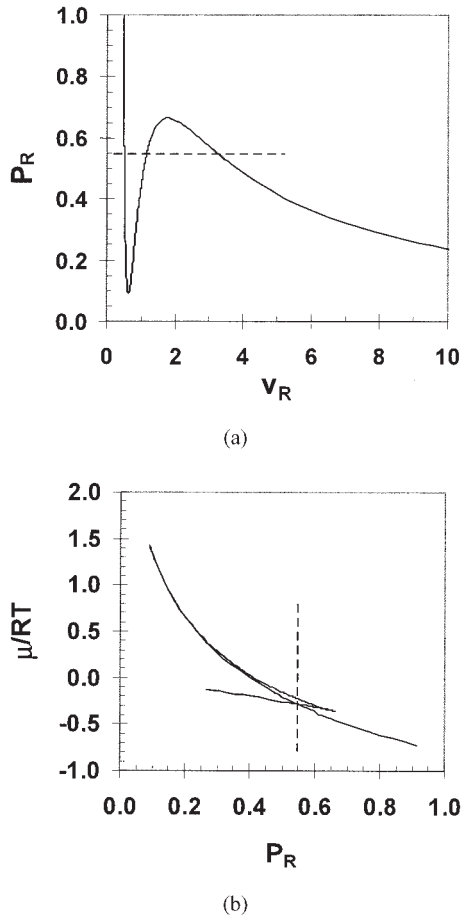

Figure 2. (a) Reduced pressure P_R as a function of reduced volume v_R at $T_R = 0.90$ for a pure fluid with $\omega = 0$, calculated using the real compressibility factor roots to the SRKEOS; (b) reduced chemical potential function μ/RT as a function of reduced pressure P_R at $T_R = 0.90$ for a pure fluid with $\omega = 0$, calculated using the real compressibility factor roots to the SRKEOS.

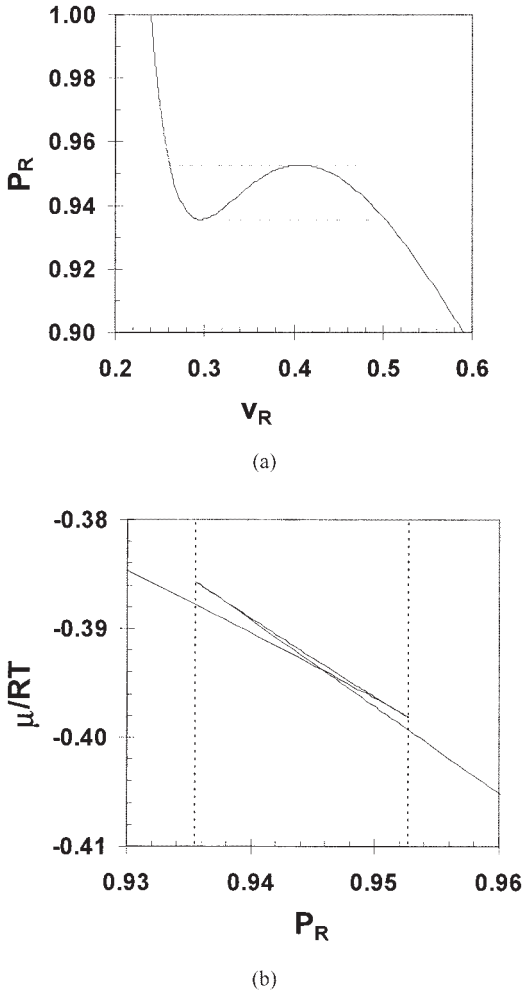

Figure 3. (a) Reduced pressure P_R as a function of reduced volume v_R at $T_R = 0.99$ for a pure fluid with $\omega = 0$, calculated using the real compressibility factor roots to the SRKEOS; (b) reduced residual chemical potential function μ/RT as a function of reduced pressure P_R at $T_R = 0.99$ for a pure fluid with $\omega = 0$, calculated using the real compressibility factor roots to the SRKEOS.

This report offers a method for finding the equilibrium state at $T_R \rightarrow 1$, which circumvents having to work only in the associated (very small) three-real-root domain. All the derivations and calculations that follow have been done with the SRKEOS; however, they are applicable to any cubic EOS.

Development

A cubic equation-of-state such as the SRKEOS

$$z^3 - z^2 + (A - B - B^2)z - AB = 0 \tag{4}$$

where z is the compressibility factor, and $A = aP/(RT)^2$ and $B = bP/RT$ are reduced EOS parameters, can be solved analytically for its three roots, which present themselves as either (1) three real roots or (2) one real root (z_1) and two complex conjugate roots (z_2 and z_3 or $z_{2,3}$). As indicated earlier, the three-real-root domain offers three sets of properties, the appropriate (stable) one of which can be identified by Second Law considerations—herein, the Gibbs minimum principle. In Figure 3a, one can identify the points at which the transition between the three-real-root and one-real-root domains occurs. For example, as one moves with decreasing v from the three-real-root domain to the one-real-root domain at z_{MIN} corresponding to P_{MIN} of the loop, two of the real z-roots become identical in value and then these z-roots become complex conjugates of each other, $z_{Re} \pm z_{Im}$, where z_{Im} is zero at the transition point and relatively small in the one-real-root domain near the transition point.

If one chooses to work with the coordinates μ–P of Figure 3b when locating the equilibrium point, one can calculate values of μ for both real and complex values of z obtained from Eq. 4. For the SRKEOS, the dimensionless residual chemical potential function μ/RT is

$$\left(\frac{\mu}{RT}\right)^{\text{resid}} = -\ln z + z - 1 - \ln\left(\frac{z-B}{z}\right) - \frac{A}{B}\ln\left(\frac{z+B}{z}\right) \tag{5}$$

The residual chemical potential function can be used in the context of Eq. 1 for finding the equilibrium state at a given T_R. Equation 5 is equal to $\ln \phi$, where ϕ is the fugacity coefficient. If z is a complex number, then one can construct $(\mu/RT)_i^{\text{resid}}$ ($i = 1$, 2, and 3), where one can obtain complex conjugate expressions

$$\left(\frac{\mu}{RT}\right)_{2,3}^{\text{resid}} = \left(\frac{\mu}{RT}\right)_{\text{Re}}^{\text{resid}} \pm i\left(\frac{\mu}{RT}\right)_{\text{Im}}^{\text{resid}} \tag{6}$$

from the two complex conjugate roots z_2 and z_3. The real and imaginary contributions to Eq. 6 can be readily obtained by expressing $z_{2,3}$ as

$$z_{2,3} = re^{\pm i\theta} \tag{7}$$

where

$$r = \sqrt{z_{\text{Re}}^2 + z_{\text{Im}}^2}$$
$$\theta = \tan^{-1}\left(\frac{z_{\text{Im}}}{z_{\text{Re}}}\right) \tag{8}$$

It follows that

$$\left(\frac{\mu}{RT}\right)_{\text{Re}}^{\text{resid}} = -\ln r' + z_{\text{Re}} - 1 - \left(\frac{A}{B}\right)\ln\left(\frac{r''}{r}\right) \tag{9}$$

$$\left(\frac{\mu}{RT}\right)_{\text{Im}}^{\text{resid}} = -\theta' + z_{\text{Im}} - \left(\frac{A}{B}\right)(\theta'' - \theta) \tag{10}$$

where

$$r' = \sqrt{(z_{\mathrm{Re}} - B)^2 + z_{\mathrm{Im}}^2}$$
$$\theta' = \tan^{-1}\left(\frac{z_{\mathrm{Im}}}{(z_{\mathrm{Re}} - B)}\right)$$
$$r'' = \sqrt{(z_{\mathrm{Re}} + B)^2 + z_{\mathrm{Im}}^2}$$
$$\theta'' = \tan^{-1}\left(\frac{z_{\mathrm{Im}}}{(z_{\mathrm{Re}} + B)}\right) \tag{11}$$

It will be shown here that one can benefit from exploiting the complex nature of a cubic EOS to expedite the computation of the equilibrium point at temperatures $T_R \rightarrow 1$, where the three-real-root domain offers very little extent with which to operate an iterative convergence routine between $(\mu/RT)^{\mathrm{resid}}$ branches so as to compute the self-intersection [equilibrium] point. The idea of exploiting complex variable space in thermodynamics is not new. Lucia and Taylor[3] demonstrated the utility of solving EOS-based vapor–liquid flash calculations in the complex domain to aid in their convergence. Some of these flash problems proved intractable in the real domain by failing to preserve distinct vapor- and liquid-phase properties for the two equilibrium phases during the convergence routine, a failure that leads to an undesired trivial solution. Lucia and Taylor would suggest that a property of a hypothetical phase obtained from complex space z can suitably be represented by the modulus of the property. In our particular application, the size of the imaginary part of $(\mu/RT)^{\mathrm{resid}}$ is small compared to the real part, and we found that $(\mu/RT)^{\mathrm{resid}}_{\mathrm{Re}}$ and $(\mu/RT)^{\mathrm{resid}}_{\mathrm{MOD}}$ differed by $<1\%$ even well away from the three-real-root domain. Its substitution had an insignificant effect on the convergence scheme.

Demonstration

Because we use the geometry of one-real-root domains as well as that of the three-real-root domain, the iterative solution seeking the equilibrium point does not require locating the pressure extrema of the subcritical van der Waals loop. No finesse is required to initiate the search for the self-intersection of the μ–P curve. We used a Newton–Raphson search for the self-intersection at a specified value of T_R, whereby the pressure of self-intersection is iteratively determined according to

$$P_{i+1} = P_i - \left.\frac{F(P)}{dF/dP}\right|_{P=P_i} \tag{12}$$

The objective function is the condition of self-intersection. When one guesses a value P_i at T_R, one obtains either one real z-root or three real z-roots from Eq. 4.

(1) If there are three real roots, they are specified $z_{(\mathrm{MIN})}$, $z_{(\mathrm{MID})}$, and $z_{(\mathrm{MAX})}$, based on the relative size of the three values of $(\mu/RT)^{\mathrm{resid}}$ computed from Eq. 5. Thus, $z_{(\mathrm{MAX})}$ is the compressibility factor of the intrinsically unstable state, and the self-intersection occurs when

$$F(P) = 0 = \left(\frac{\mu}{RT}\right)^{\mathrm{resid}}\Bigg|_{z_{(\mathrm{MID})}} - \left(\frac{\mu}{RT}\right)^{\mathrm{resid}}\Bigg|_{z_{(\mathrm{MIN})}} \tag{13}$$

(2) If there is one real root, it corresponds to $z_{(\mathrm{MIN})}$. The objective function in Eq. 13 becomes

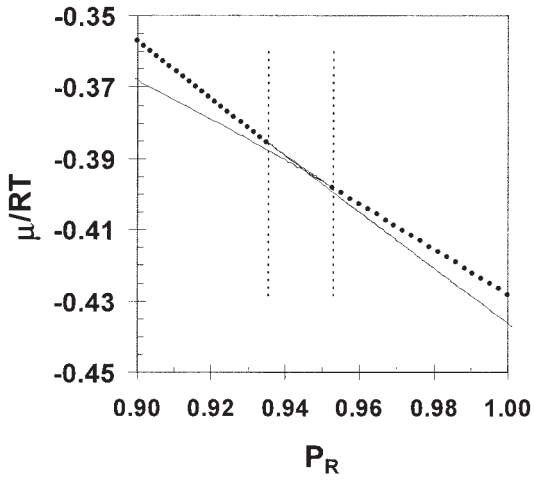

Figure 4. Same as Figure 3b, with the addition of the real part of the reduced residual chemical potential function μ/RT in the one-real-root domain (denoted by bold dots), calculated using the complex conjugate roots to the SRKEOS.

$$F(P) = 0 = \left(\frac{\mu}{RT}\right)^{\mathrm{resid}}_{\mathrm{Re}} - \left(\frac{\mu}{RT}\right)^{\mathrm{resid}}\Bigg|_{z_{(\mathrm{MIN})}} \tag{14}$$

where the first term on the right-hand side is Eq. 9. The pressure derivative dF/dP is analytically obtainable from either Eq. 13 or 14, and so Eq. 12 is analytically expressible.

Because z_{Im} is small near and vanishes at the three-real-root to one-real-root transition points, it follows that $(\mu/RT)^{\mathrm{resid}}_{\mathrm{Im}}$ does also. Figure 4 superimposes $(\mu/RT)^{\mathrm{resid}}_{\mathrm{Re}}$ (Eq. 9) on the curves of Figure 3b. The real part of Eq. 6 extends in a well-behaved manner to pressures well beyond those shown in Figure 4.

Tables 1 and 2 demonstrate how effectively this iterative routine works. In Table 1, the SRKEOS for $\omega = 0$ is solved for the saturation pressure at various T_R-values: 0.95, 0.99, 0.9999, and 0.999999. Each search is initiated with the (intentionally poor) value of $P_R = 0.1$. Convergence is successfully obtained in all cases in relatively rapid style. Table 1 notes with each iterative step whether the search is in the one-real-root or three-real-root domain. Table 2 repeats these calculations for $\omega = 1$. In passing it should be noted that the initiation does not have to be $P_R < 1$. The domain over which this strategy works is especially large to both sides of the equilibrium result.

Conclusion

By examining all the roots provided by the analytical solution to a cubic EOS, one can exploit information provided by the complex conjugate roots in the one-real-root domain and compute equilibrium states near the critical point without having to identify a reasonable initial guess for the iterative procedure.

Notation

A = reduced a-parameter of the SRKEOS
B = reduced b-parameter of the SRKEOS

Table 1. Convergence Behavior for Calculation $P_{R,sat}$ at T_R = 0.95, 0.99, 0.9999, and 0.999999 for an SRKEOS Fluid with ω = 0*

ω = 0 Iteration	T_R = 0.95 P_R	Difference	Root Domain	T_R = 0.99 P_R	Difference	Root Domain	T_R = 0.9999 P_R	Difference	Root Domain	T_R = 0.999999 P_R	Difference	Root Domain
Initiation	0.100000		1	0.100000		1	0.100000		1	0.100000		1
1	0.266795	1.67E-01	1	0.280685	1.81E-01	1	0.283952	1.84E-01	1	0.283984	1.84E-01	1
2	0.488616	2.22E-01	1	0.539855	2.59E-01	1	0.552261	2.68E-01	1	0.552384	2.68E-01	1
3	0.662118	1.74E-01	3	0.762932	2.23E-01	1	0.787823	2.36E-01	1	0.788072	2.36E-01	1
4	0.736638	7.45E-02	3	0.885022	1.22E-01	1	0.920385	1.33E-01	1	0.920738	1.33E-01	1
5	0.748842	1.22E-02	3	0.931894	4.69E-02	1	0.974202	5.38E-02	1	0.974623	5.39E-02	1
6	0.749198	3.56E-04	3	0.945180	1.33E-02	3	0.992108	1.79E-02	1	0.992570	1.79E-02	1
7	0.74919787	3.10E-07	3	0.945830	6.50E-04	3	0.997442	5.33E-03	1	0.997932	5.36E-03	1
8	0.7491978680	2.35E-13	3	0.945833	3.42E-06	3	0.998929	1.49E-03	1	0.999438	1.51E-03	1
9				0.94583338	9.96E-11		0.999322	3.93E-04	1	0.999844	4.07E-04	1
10				0.9458333777	6.44E-15		0.999420	9.74E-05	1	0.999951	1.07E-04	1
11							0.999441	2.09E-05	3	0.999979	2.75E-05	1
12							0.99944154	9.88E-07	3	0.999986	6.95E-06	1
13							0.999441544	2.87E-10	3	0.999987	1.71E-06	1
14							0.9994415435	3.00E-14	3	0.999988	3.95E-07	1
15										0.99998786	7.57E-08	3
16										0.99998785	−4.03E-09	3
17										0.999987854	1.45E-12	3
18										0.999987854	−1.32E-13	3

*In each case, an initial guess of P_R = 0.1 is used.

Table 2. Convergence Behavior for Calculation $P_{R,sat}$ at T_R = 0.95, 0.99, 0.9999, and 0.999999 for an SRKEOS Fluid with ω = 1*

ω = 1.00 Iteration	T_R = 0.95 P_R	Difference	Root Domain	T_R = 0.99 P_R	Difference	Root Domain	T_R = 0.9999 P_R	Difference	Root Domain	T_R = 0.999999 P_R	Difference	Root Domain
Initiation	0.100000		1	0.100000		1	0.100000		1	0.100000		1
1	0.254316	1.54E-01	3	0.278398	1.78E-01	1	0.283930	1.84E-01	1	0.283984	1.84E-01	1
2	0.441556	1.87E-01	3	0.531146	2.53E-01	1	0.552174	2.68E-01	1	0.552383	2.68E-01	1
3	0.561238	1.20E-01	3	0.745232	2.14E-01	1	0.787646	2.35E-01	1	0.788070	2.36E-01	1
4	0.593544	3.23E-02	3	0.859290	1.14E-01	1	0.920129	1.32E-01	1	0.920736	1.33E-01	1
5	0.595563	2.02E-03	3	0.900218	4.09E-02	3	0.973891	5.38E-02	1	0.974620	5.39E-02	1
6	0.595570	7.62E-06	3	0.905642	5.42E-03	3	0.991760	1.79E-02	1	0.992567	1.79E-02	1
7	0.59557049	1.08E-10	3	0.905768	1.26E-04	3	0.997069	5.31E-03	1	0.997928	5.36E-03	1
8	0.5955704924	−8.88E-16	3	0.90576801	7.53E-08	3	0.998537	1.47E-03	1	0.999434	1.51E-03	1
10				0.9057680132	2.15E-14	3	0.998917	3.80E-04	1	0.999840	4.06E-04	1
11							0.999005	8.77E-05	3	0.999947	1.07E-04	1
12							0.999015	1.04E-05	3	0.999975	2.75E-05	1
13							0.99901492	−3.49E-08	3	0.999981	6.91E-06	1
14							0.9990149173	5.26E-13	3	0.999983	1.68E-06	1
15										0.999984	3.78E-07	3
16										0.99998359	5.40E-08	3
17										0.99998358	−1.15E-09	3
18										0.9999835848	1.17E-13	3

*In each case, an initial guess of P_R = 0.1 is used.

F = objective function for finding pure-component phase equilibrium
G = Gibbs energy
P = pressure
r = amplitude of the complex conjugate compressibility factor
R = gas constant
T = temperature
v = molar volume
z = compressibility factor

Greek letters

μ = pure-component chemical potential function (molar Gibbs energy)
ω = acentric factor
θ = angle associated with the complex conjugate compressibility factor

Subscripts

g = gas phase
Im = imaginary part
l = liquid phase
MIN = minimum
MID = middle
MAX = maximum
R = reduced
Re = real part
1, 2, 3 = labels of compressibility factor roots to the SRKEOS

Superscript

resid = residual, or departure, contribution

Literature Cited

1. Soave G. Equilibrium constants from a modified Redlich–Kwong equation-of-state. *Chem Eng Sci.* 1972;27:1197-1203.
2. Peng DY, Robinson DB. A new two-constant equation of state. *Ind Chem Eng Fundam.* 1976;15:59-64.
3. Lucia A, Taylor R. Complex iterative solutions to process model equations? *Comput Chem Eng.* 1992:16S:387-394.

Manuscript received Sept. 29, 2004, and revision received Nov. 14, 2005.